LAWRENCE
LIVERMORE
NATIONAL
LABORATORY

LLNL-JRNL-717099

Rapid feedback of chemical vapor deposition growth mechanisms by operando x-ray diffraction

A. A. Martin, P. J. Depond, M. Bagge-Hansen, J. R .I. Lee, J. H. Yoo, S. Elhadj, M. J. Matthews, T. van Buuren

January 9, 2017

Journal of Vacuum Science and Technology B

Disclaimer

Rapid feedback of chemical vapor deposition growth mechanisms by operando X-ray diffraction

Aiden A. Martin, Philip J. Depond, Michael Bagge-Hansen, Jonathan R.I. Lee,
Jae-Hyuck Yoo, Selim Elhadj, Manyalibo J. Matthews, and Tony van Buuren*
Physical and Life Sciences Directorate, Lawrence Livermore National Laboratory, Livermore, California 94550, USA
(Dated: February 22, 2018)

An operando X-ray diffraction system is presented for elucidating optimal laser assisted chemical vapor deposition growth conditions. The technique is utilized to investigate deposition dynamics of boron-carbon materials using trimethyl borate precursor. Trimethyl borate exhibits vastly reduced toxicological and flammability hazards compared to existing precursors but has previously not been applied to boron carbide growth. Crystalline boron-rich carbide material is produced in a narrow growth regime on addition of hydrogen during the growth phase at high temperature. The use of the operando X-ray diffraction system allows for the exploration of highly non-equilibrium conditions and rapid process control, which are not possible using ex situ diagnostics.

Laser assisted chemical vapor deposition (L-CVD) provides the means to deposit high quality, crystalline and conformal films with a high degree of spatial control. In the pyrolytic mode of L-CVD, selective deposition of material is achieved by thermally decomposing gaseous precursors using localized laser heating of a substrate [1]. The ability to control the location of the deposit enables the fabrication of films with complex structures, including materials with gradiated compositions (both laterally and vertically) and asymmetric properties [2–4].

Fully harnessing the capabilities of L-CVD requires a detailed understanding of the relationship between the structure/composition of the deposit and the process conditions. Identifying these relationships using ex situ, Edisonian, approaches is an arduous process, involving exploration of a matrix of numerous parameters that include the substrate temperature, laser profile, and gas compositions and pressure [5]. The development of in situ/operando structural diagnostics is, therefore, essential for the rapid evaluation of the effects of varying deposition conditions; furthermore, operando methods also provide the potential for exploring highly non-equilibrium conditions and the possibility of real-time process control, which are not possible using ex situ diagnostics. This work expands on previous in situ X-ray studies of chemical vapor deposition [6, 7], with the incorporation of laser induced heating to localize the growth zone on the substrate.

In this paper, the development and use of a system for the operando X-ray diffraction (XRD) characterization of L-CVD grown thin films is reported. Boron carbide materials were selected in this study for two important reasons: (1) this class of materials exhibit ultrahard and radiological properties that have a range of technological uses but are challenging to deposit via conventional methods, particularly with precise control over the location of the film [8], and (2) a potential new precursor gas, trimethyl borate (TMB, $B(OCH_3)_3$) [9, 10], has been identified for CVD that is vastly less toxic and flammable than traditional precursors (such as $B(CH_3)_3$ [11], $B(C_2H_5)_3$ [12], BCl_3 and B_2H_6 [8]). The availability of a less hazardous precursor is significant because understanding the processes of boron carbide formation using TMB could lead to routine use that would enhance safety and, by extension, could improve the economics of boron based coatings for numerous applications.

The operando XRD system for time resolved measurement of crystalline material growth during L-CVD is based on a Kimball Physics 8" Spherical Square ultra high-vacuum chamber. The chamber contains an optically transparent window for laser admittance and two beryllium windows for admittance and egress of x-rays (Fig. 1). A 532 nm continuous wave laser (5 W, Sprout-D, Lighthouse Photonics) was focused to a Gaussian beam radius (ω_0) of $\sim$ 475 μm and irradiated the substrate at a 75° angle of incidence to generate localized heat in the substrate. Mixtures of TMB and hydrogen were used as material growth precursors. Three temperature regimes were studied using varied substrate parameters to enable the heating profiles. Copper coated (20 nm copper on 5 nm titanium) 8% yttria-stabilized zirconia (YSZ, MTI Corporation) substrates were used as the growth platform at low (2.63 W laser power) and intermediate (2.98 W laser power) temperatures as they provided effective coupling of the incident laser light to reach controlled temperatures. For the high temperature regime, amorphous carbon coated (20 nm) 8% yttria-stabilized zirconia substrates were used as the growth platform to provide maximum light coupling. To further increase the temperature the system was also reconfigured to provide a laser angle of incidence of $\sim 10°$ during these growths while maintaining a laser power of 2.98 W.

Calculation of the steady state substrate temperature for low and intermediate experimental L-CVD conditions was performed using the COMSOL Multiphysics software package [13]. The thermal conductivity (k), specific heat capacity (C) and density (ρ) parameters for copper, titanium, and YSZ substrate components were assumed to equal their bulk values in the calculations [14]. As the

* vanbuuren1@llnl.gov

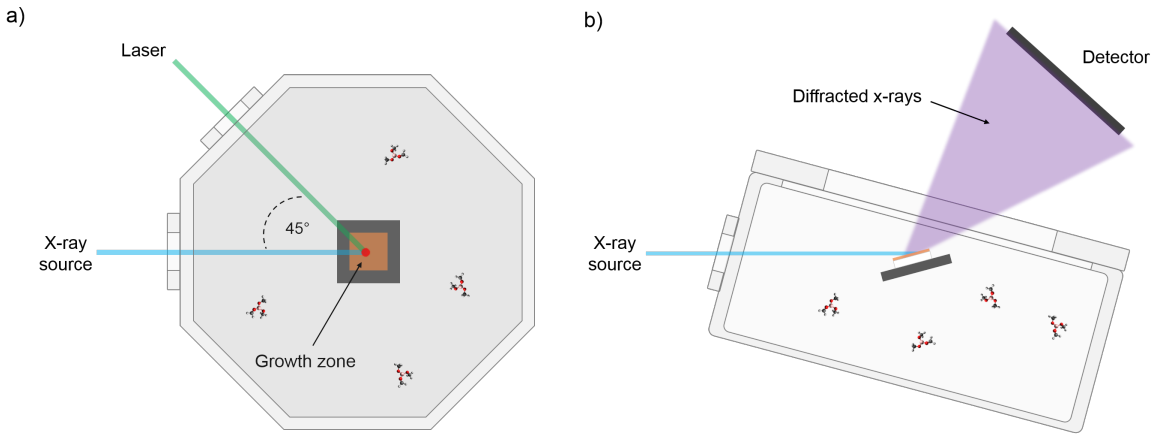

FIG. 1. (Color online) (a) Top and (b) side view schematic illustrations of the L-CVD growth and operando XRD measurement system. The system consists of a 532 nm laser and focusing optics, pumping system (not shown), gas inlet, specimen stage, beryllium X-ray windows and quartz optical window. (a) The laser used for localized heating of the substrate and synchrotron X-ray radiation are coincident on the substrate surface. (b) X-rays diffracted by the substrate material egress through a top mounted beryllium window and are collected on a PilatusII 100K area detector.

substrates had a high surface roughness (R_a = 50 μm) and the substrate is rapidly covered in carbonaceous material upon heating, the optical reflectivity of the surface was set to zero. The substrate was mounted to an aluminum stage which we assume was at room temperature during the experiments. The minimum substrate temperature in the high temperature regime was determined by the shift of the YSZ (111) d-spacing measured during growth. The 0.033 Å change in d-spacing corresponds to a temperature of $\sim$ 1200 °C [15]. The carbon film is certainly at a considerably higher temperature than 1200 °C given that it directly couples to the laser and has poor thermal conductivity; however, this shift in substrate d-spacing gives the best experimental approximation of the growth temperature.

XRD measurements were performed on beamline 33-ID-D at the Advanced Photon Source, Argonne National Laboratory using 8 kV x-rays (1.514 Å). Incident x-rays were aligned to be coincident with the laser on the sample surface to probe the L-CVD growth region and the diffracted X-ray signal was collected in the 2θ region of 20 - 60° by a PilatusII 100K area detector. The X-ray beam spot was approximately 1,000 × 100 μm in size and irradiated a surface area of 1,000 × 386 μm at the 75° angle of incidence used during the experiments. Therefore the entire cross-section of the deposit was probed by XRD during growth. A well-defined procedure was performed via sequential steps for material growth and operando measurement. (i) from atmosphere the vacuum chamber was pumped until high-vacuum was obtained ($\leq 10^{-4}$ Torr), (ii) TMB precursor and hydrogen (if required) were admitted into the vacuum chamber, (iii) an initial XRD pattern of the substrate was collected, (iv) the laser was then turned on and sequential XRD patterns were collected until growth was halted by turning off the laser. Each XRD pattern collection in the low and intermediate temperature regime required $\sim$ 4 minutes, with the measurement sequentially acquired in the region where the majority of boron-carbon material diffraction peaks were anticipated: from 20 to 60° in 2θ.

Postmortem analysis of each deposit was performed ex situ using Raman and energy dispersive X-ray spectroscopy (EDS) to determine their steady state structure and atomic composition. Raman spectroscopy was performed using a Thermo Scientific Nicolet Almega XR micro-Raman system using a 633 nm, 1 mW laser and a 50× magnification, 0.5 NA objective lens. EDS was performed using a Phenom ProX scanning electron microscope (SEM) at 5 keV electron energy.

As an initial stage of analysis, the XRD patterns were calibrated by a linear fitting function using known YSZ peak positions (2θ: 30.269, 35.084, 50.459, 59.994 °) [16] to account for small misalignments in the experimental geometry before applying a Sonneveld-Visser baseline subtraction routine. The collected XRD spectra showed major diffraction lines attributed to YSZ and copper in the region $2\theta > 30°$ and a minor peak attributed to YSZ at $\sim$ 24.6°. This is advantageous for our measurement because boron carbide species typically exhibit a number of diffraction peaks in the range from 20 to 26°, where there are minimal contributions from YSZ.

The composition of the crystalline component formed during material growth was determined by XRD fingerprinting using the ICDD PDF4+ powder diffraction database [17]. The database contains > 380,000 material entries, each of which was compared directly to our collected spectra after linear and baseline correction. Rietveld refinement was not performed due to the low in-

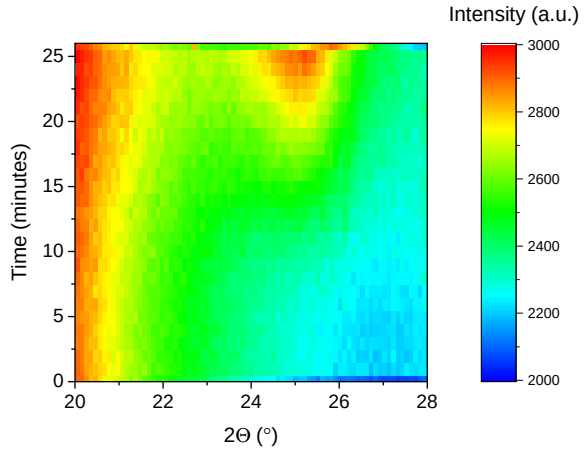

FIG. 2. (Color online) Contour plot of XRD patterns collected as a function of time during L-CVD material growth using 50 Torr of TMB and 50 Torr of hydrogen as the precursor material, and a substrate temperature > 1200 °C. Values at zero minutes indicate the XRD pattern of the substrate before laser induced heating was applied. Time axis indicates the total time the laser had been on at the end of the corresponding scan. Laser irradiation was terminated at 26 minutes resulting in substrate cooling and the observed shift in peak positions.

tensity of peaks associated with nascent ultra-hard film growth and the fact that large substrate peaks dominate in large regions of the diffraction pattern. Instead, fingerprinting was used to match the peak positions of deposits of unknown composition to the extensive number of known compounds within the PDF4+ library. A particular emphasis during fingerprinting was placed upon materials composed of elements known to be present in the reaction environment, specifically copper, titanium, carbon and 8%-YSZ from the substrate material and boron, oxygen, carbon and nitrogen from the deposited material. Mixtures of elements with copper and titanium were considered even though the peaks associated with these materials in the samples were likely to be broad due to finite size effects [18].

To determine the effectiveness of the technique to measure material growth with meaningful resolutions, initial L-CVD/XRD measurements were performed under conditions known to lead to deposition: 50 Torr of TMB and 50 Torr of hydrogen as the precursor material in the high temperature regime (calculated temperature > 1200 °C). Fig. 2 provides a clear indication of the effectiveness of the technique as it displays the XRD patterns collected as a function of L-CVD growth time under these conditions. Growth of material is quickly detected with a major amorphous diffraction peak appearing at ∼ 25 °, and no evidence of crystalline material growth during substrate heating or subsequent cooling.

Additional operando measurements during L-CVD were performed to provide new insight into the material growth mechanism for thin film boron carbides using

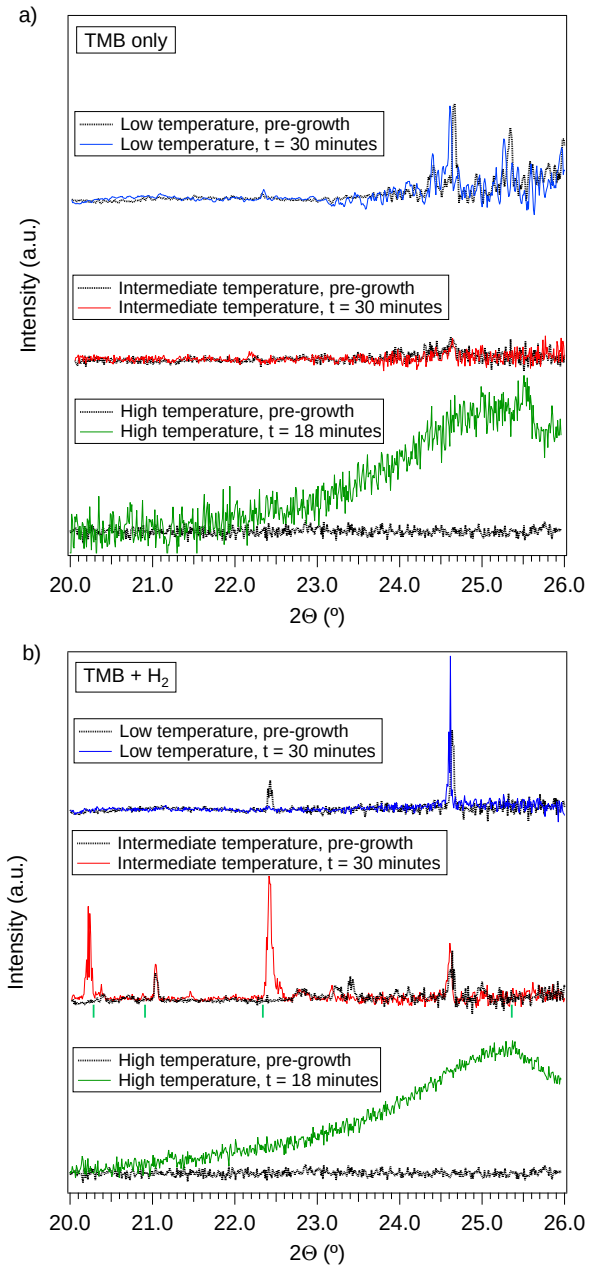

FIG. 3. (Color online) Operando XRD patterns collected prior to (dashed) and during (solid) L-CVD material growth. (a) Growth with TMB precursor only using 10 Torr of TMB in the low temperature regime, 20 Torr in the intermediate temperature regime, and 50 Torr TMB in the high temperature regime. (b) Growth with TMB and hydrogen as the precursor material using 10 Torr of TMB and 42 Torr of hydrogen in the low and intermediate temperature regimes, and 50 Torr of TMB and 50 Torr of hydrogen in the high temperature regime. (–) Ticks indicate position of B_8C diffraction lines, with major peaks at ∼ 20.3 and 22.35°. The peak at 24.6° originates from the YSZ substrate.

TMB precursor, via variation in the heating conditions and the pressure and composition of the reactant gases. First, L-CVD was performed in the absence of hydrogen,

using 10 Torr of TMB and a laser power of 2.63 W, and 20 Torr of TMB and a laser power of 2.98 W (Fig. 3a). Growth of crystalline material is not evident in the XRD pattern and the cause is ascribed to deposition of amorphous material containing boron, oxygen and/or carbon in the gradated heating zone. This is consistent with other systems such as diamond where hydrogen drives crystallization through removal of deposited amorphous phases, activation of reaction pathways between the precursor and substrate, and reaction between precursor and hydrogen in the gas phase [19, 20]. The addition of hydrogen may enable pathways for preventing the formation of oxides, such as the formation of water as a parallel reaction path. Additionally, hydrogen could enable the formation of boric acid (H_3BO_3) and methane via reaction with the TMB precursor. Heating of boric acid leads to the formation of boron trioxide (B_2O_3) material which is stable at lower temperatures and could indicate why oxygen content is high in the films. In high-temperature regions boric acid or boron trioxide can be reduced through a carbothermic process or via metal induced reduction by the underlying copper-titanium film [21]. This could be further aided by hydrogen reducing any metal oxide or boron suboxides formed during the process. The reduction of boron oxide and formation of boron carbide material is complex and requires a future in-depth study now that favorable conditions have been identified in this system.

Depositions with hydrogen were performed using 10 Torr of TMB and 42 Torr of hydrogen as the precursor material, but with varying laser powers (2.63 and 2.98 W respectively) (Fig. 3b). At a laser power of 2.63 W growth of crystalline material was not observed. A transition in growth profiles is observed upon increasing the laser power from 2.63 to 2.98 W (peak temperature ~ 680 to ~ 770 °C) resulting in growth of crystalline material. Growth of crystalline material is quickly detected with major diffraction peaks appearing at 20.22 and 22.41° and minor peaks at 20.38, 20.88, 21.46 and 22.55°. XRD peaks observed in the material during growth are consistent with the deposition of a boron-rich carbide material, with B_8C [22] providing the closest match to peaks observed over the range of 2θ measured. Other materials composed of elements present in the reaction environment that could lead to peaks in the 20-26° range, such as boron oxides, did not provide as close a match as B_8C; moreover, deposits of these materials are generally amorphous and occur in the crystalline phase only under high pressure and temperature conditions. B [23], $B_{11.4}C_{3.6}$ [24], B_4C [25] and $B_{10.4}C_{1.6}$ [24] were also considered however these did not represent a good match to the collected data.

The assignment of B_8C is significant because it is a metastable material [26, 27] that would not be observed ex situ. This clearly demonstrates that the operando XRD measurement system is ideal for the study of L-CVD growth under thermodynamically challenging and non-equilibrium conditions. Further studies using the operando XRD approach could probe thermodynamic properties of materials where the material undergoes a phase change or new crystallographic features emerge during growth, which could yield identification of new structures at high temperature. As shown here it can be harnessed to promptly find these conditions in a previously unexplored system. Note that the deposit is not pure, stoichiometric B_8C throughout its entire lateral cross section due to thermal gradients induced by laser heating; nonetheless, the non-uniform heating allows for material growth under a range of temperatures within the deposit which can be probed simultaneously via XRD. Laser heating therefore allows rapid probing of a new precursor to determine if favorable conditions are present anywhere in the system.

Finally, depositions were performed using 50 Torr TMB with and without the presence of 50 Torr of hydrogen with a laser power of 2.98 W and an angle of incidence of 10 °. In this high temperature (> 1200 °C) growth regime both deposits were amorphous in structure with broad features centered around 25 ° in the collected XRD pattern. This regime also brought about notable changes to the YSZ substrate which were not observed int he other growth regimes. This allowed for the experimental determination of a minimum substrate temperature based on the shift in the YSZ substrate peak position.

Postmortem analysis of the deposits reveals interesting differences between the deposits fabricated at intermediate and high temperatures. Raman spectroscopy indicates a mixture of single crystal and amorphous material at the intermediate growth regime with the addition of hydrogen while deposits formed in the high temperature regime display graphitic carbon characteristics. Analysis of the material by EDS shows further differences between the two growth regimes. The intermediate growth deposit where B_8C material was detected contains boron, carbon and oxygen while the higher temperature regime deposit only contains carbon. Regions of material with high concentrations of boron and carbon were detected via SEM and EDS, however, these areas where oxidized and therefore accurate determination of the material stoichiometry in these regions was not possible. The surface temperature in the high temperature regime was therefore hot enough to efficiently desorb boron and oxygen from the surface via a thermally induced pathway such as sublimation of boron oxide. The presence of oxygen in the intermediate growth deposit is ascribed to the large thermal gradient present across the profile which varies the local growth conditions.

In conclusion, operando XRD measurements were used to characterize L-CVD material growth using a TMB precursor under varied precursor environment and three distinct temperature regimes. The presence of hydrogen at elevated temperature was shown to be critical in the production of boron-rich carbide material. Exceeding this temperature resulted in deposition of amorphous carbon material with complete removal of boron and oxygen from the thin film. The ability to observe crystal

phase changes during operation allows the characterization of transient and metastable phases that would not be observed ex situ and limits the need for arduous processing routines. These results demonstrate a platform for accelerated implementation of novel CVD precursor systems and a method for process control under conventional growth recipes.

This work was performed under the auspices of the U.S. Department of Energy (DOE) by Lawrence Livermore National Laboratory (LLNL) under Contract DE-AC5207NA27344. Project 14-ERD-067 was funded by the LDRD Program at LLNL. This research used resources of the Advanced Photon Source, a U.S. DOE Office of Science User Facility operated for the DOE Office of Science by Argonne National Laboratory under Contract No. DE-AC02-06CH11357. The authors gratefully acknowledge the experimental support (XRD) of Z. Zhang (Advanced Photon Source, Argonne National Laboratory).

REFERENCES

[1] D. J. Ehrlich and J. Y. Tsao, J. Vac. Sci. Technol., B: Nanotechnol. Microelectron.: Mater., Process., Meas., Phenom. **1**, 969 (1983).
[2] O. Lehmann and M. Stuke, Mater. Lett. **21**, 131 (1994).
[3] M. C. Wanke, O. Lehmann, K. Müller, Q. Wen, and M. Stuke, Science **275** (1997).
[4] J. Yeo, S. Hong, M. Wanit, H. W. Kang, D. Lee, C. P. Grigoropoulos, H. J. Sung, and S. H. Ko, Adv. Funct. Mater. **23**, 3316 (2013).
[5] F. A. Houle, Appl. Phys. A: Solids Surf. **41**, 315 (1986).
[6] M. I. Richard, M. J. Highland, T. T. Fister, A. Munkholm, J. Mei, S. K. Streiffer, C. Thompson, P. H. Fuoss, and G. B. Stephenson, Appl. Phys. Lett. **96**, 051911 (2010).
[7] G. Ju, M. J. Highland, A. Yanguas-Gil, C. Thompson, J. A. Eastman, H. Zhou, S. M. Brennan, G. B. Stephenson, and P. H. Fuoss, Rev. Sci. Instrum. **88**, 035113 (2017).
[8] A. K. Suri, C. Subramanian, J. K. Sonber, and T. S. R. C. Murthy, Int. Mater. Rev. **55**, 4 (2010).
[9] H. Sachdev, F. Müller, and S. Hüfner, Angew. Chem., Int. Ed. Engl. **50**, 3701 (2011).
[10] F. Müller, M. Lessel, S. Grandthyll, K. Jacobs, S. Hüfner, S. Gsell, M. Weinl, and M. Schreck, Langmuir **29**, 4543 (2013).
[11] M. Imam, L. Souqui, J. Herritsch, A. Stegmüller, C. Höglund, S. Schmidt, R. Hall-Wilton, H. Högberg, J. Birch, R. Tonner, and H. Pedersen, J. Phys. Chem. C **121**, 26465 (2017).
[12] M. Imam, K. Gaul, A. Stegmüller, C. Höglund, J. Jensen, L. Hultman, J. Birch, R. Tonner, and H. Pedersen, J. Mater. Chem. C **3**, 10898 (2015).
[13] M. J. Matthews, S. Elhadj, G. M. Guss, A. Sridharan, N. D. Nielsen, J.-H. Yoo, D. Lee, and C. Grigoropoulos, in *Proc. SPIE 8885, Laser-Induced Damage in Optical Materials: 2013*, edited by G. J. Exarhos, V. E. Gruzdev, J. A. Menapace, D. Ristau, and M. Soileau (2013) p. 888526.
[14] Thermal properties: copper (k = 400 W m^{-1} K^{-1}, C = 385 J kg^{-1} K^{-1}, ρ = 8,960 kg m^{-3}), titanium (k = 21.9 W m^{-1} K^{-1}, C = 544 J kg^{-1} K^{-1}, ρ = 4,506 kg m^{-3}), YSZ (k = 1.26 W m^{-1} K^{-1}, C = 470 J kg^{-1} K^{-1}, ρ = 5,813 kg m^{-3}).
[15] E. Coker, M. Rodriguez, A. Ambrosini, J. Miller, and E. Stechel, Powder Diffr. **27**, 117 (2012).
[16] Pfoertsch and McCarthy, *ICDD Grant-in-Aid* (Penn State University, University Park, Pennsylvania, USA, 1977).
[17] T. G. Fawcett, J. Faber, S. Kabbekodu, F. Mcclune, and D. Rafaja, in *Microstructure Analysis in Materials Science* (Freiberg, 2005) pp. 1–3.
[18] J. I. Langford and A. J. C. Wilson, J. Appl. Crystallogr. **11**, 102 (1978).
[19] Y. Matsui and M. Sahara, Jpn. J. Appl. Phys. **28**, 1023 (1989).
[20] M. Frenklach and H. Wang, Phys. Rev. B **43**, 1520 (1991).
[21] A. Atasoy, Int. J. Refract. Met. Hard Mater. **28**, 616 (2010).
[22] K. Ploog, J. Cryst. Growth **24**, 197 (1974).
[23] B. Callmer and IUCr, Acta Crystallogr., Sect. B: Struct. Crystallogr. Cryst. Chem. **33**, 1951 (1977).
[24] S. V. Konovalikhin and V. I. Ponomarev, Russ. J. Inorg. Chem. **54**, 197 (2009).
[25] H. K. Clark and J. L. Hoard, J. Am. Chem. Soc. **65**, 2115 (1943).
[26] E. Amberger, W. Stumpf, and K. C. Buschbeck, *Gmelin Handbook of Inorganic Chemistry* (Springer-Verlag, Berlin, 1981).
[27] A. Velamakanni, K. J. Ganesh, Y. Zhu, P. J. Ferreira, and R. S. Ruoff, Adv. Funct. Mater. **19**, 3926 (2009).